

# RPC-IES Users Guide

## General Information

Contact:

Jim Burch, Southwest Research Institute, San Antonio, Texas USA

Email: [jburch@swri.edu](mailto:jburch@swri.edu)

Covers RPC-IES Ion and Electron data L2, L3 and L5

Revision 0

**Missing in current revision:**

TBD

## Table of Contents

<b>General Information .....</b>	<b>1</b>
Missing in current revision: .....	1
<b>Table of Contents .....</b>	<b>1</b>
<b>Scope.....</b>	<b>2</b>
<b>Conventions.....</b>	<b>2</b>
<b>Introduction.....</b>	<b>2</b>
<b>Instrument Characteristics .....</b>	<b>3</b>
<b>IES Data description .....</b>	<b>3</b>
What the data contain .....	3
<b>Calibrated data.....</b>	<b>5</b>
How to go from L2 to L3 .....	5
<b>Working with geometry data .....</b>	<b>5</b>
Coordinate systems.....	5
Working with the field of view .....	6
<b>Appendix 1.....</b>	<b>8</b>
Contents of Level 2 data .....	8
Contents of L3 data .....	9
Contents of L5 data .....	10
Figure 3. Line plots of result of moment calculations for electrons measured on 30 July 2016. ....	11

## Scope

The scope of this guide is to show how RPC-IES data can be used. It is assumed that the user can read the data from the PDS formatted data files. For details on the format the user is referred to the Experimenter to Archive Interface Control Document and the Planetary Science Archive (PSA) data labels. The format is also briefly described in Appendix 1.

The instrument is described by Burch et al. (2007). An update on the instrument characteristics compared to that document is provided in this document.

## Conventions

The instrument has 16 directional anodes, termed sectors. The angle of the field of view of a sector is referred to as the azimuthal angle. Sectors are numbered from 0 to 15.

There are likewise 16 elevation steps, corresponding to the angle of the look direction out of the detector symmetry plane. We refer to this angle as the elevation angle. Elevations are numbered from 0 to 15.

## Introduction

RPC-IES is a dual electrostatic analyzer onboard the Rosetta spacecraft. It is a part of the Rosetta Plasma Consortium (Carr et al. 2007) which also consists of the RPC-ICA ion composition analyzer (Nilsson et al. 2007), the RPC-MAG magnetometer (Glassmeier et al. 2007), the RPC-LAP Langmuir probe (Eriksson et al. 2007) and the RPC-MIP Mutual Impedance Probe (Trotignon et al. 2007).

RPC-IES has  $2.8\pi$  angular coverage and measures electrons and positively charged ions in an energy range from 4 eV to 17 keV. Data from the electron channels is sometimes interpreted as negative ions (Burch et al., 2015a) or charged nanograins (Burch et al., 2015b) depending on the energy spectrum and other characteristics. The instrument is described in Burch et al. (2007). An updated instrument summary is given in the section Instrument Characteristics.

The data from the first encounter of Rosetta with the comet atmosphere were published in Burch et al. (2015a,b), Goldstein et al. (2015), Clark et al. (2015), and Broiles et al. (2015).

## Instrument Characteristics

The revised instrument characteristics are summarized in table 1.

**Table 1 Instrument characteristics**

Quantity		Values
Energy	Range	4 eV/e to 17 keV/e
	Resolution	$\Delta E/E = 0.08$
	Scan	128 steps
Angle	Range (FOV)	$90^\circ \times 360^\circ (2.8 \pi \text{ sr})$
	Resolution (electrons)	$5^\circ \times 22.5^\circ$ (Bin centers, 16 elevation angles x 16 azimuth angles)
	Resolution (ions)	$5^\circ \times 45^\circ$ (Bin centers, 16 elevation angles x 7 azimuth angles) $5^\circ \times 5^\circ$ (Bin centers, 16 elevation angles x 9 azimuth angles covering the $45^\circ$ sector containing the solar wind direction)
Temporal resolution	Full FOV distribution	128 s to 1024 s (mode dependent)
Geometric Factor (cm <sup>2</sup> sr eV/eV per pixel)	For ions: Anodes 0-2 and 12 -15: 6.000E-05 Anodes 3-11: 6.667E-06 For electrons: CALIB\ELC_FLIGHT_G.TAB	

## IES Data description

### What the data contain

The RPC-IES files all contain counts for one energy sample per line, with counts for each azimuth channel and additional information about instrument mode, start and stop energy, elevation angle range, cycle time, and quality flag. The data layout is summarized in Appendix 1. We will here briefly describe what these variables mean and how they can be used.

The azimuth and elevation provide the look direction of the instrument. The physical azimuth (sector) angle corresponding to a given azimuth index (0-15) is constant in the instrument frame. The elevation angle corresponding to a given elevation index value (0-15) is set by deflection voltages that are proportional to the particle energy so that the range is  $-45^\circ$  to  $45^\circ$  for all energies.

In order to avoid having too many energy steps, linear stepping with 4 eV/step is used for steps 0-24 (4.32 – 107.88 eV), and logarithmic stepping is used for the

higher energies with energy ratios varying within the range of 1.04 – 1.07. The full set of energy steps is shown in.

In order to stay within available telemetry limits data were binned onboard. How they were binned is given in [DOCUMENT\IES\\_MODES\IES\\_MODES.PDF](#). Binning is accomplished by combining adjacent values of energy, elevation angle and azimuth (abbreviated by Adj. in the Tables ). The mode number used at a particular time is given in one of the columns in the data and also in the spectrograms. Note that occasionally there was a mode change while data were recorded, leaving a short break in the data sequence..

**Table 2 The IES energy steps**

Steps	Energy (eV)				
0-4	4.32	8.63	12.95	17.26	21.58
5-9	25.89	30.21	34.52	38.84	43.15
10-14	47.47	51.78	56.10	60.41	64.73
15-19	69.04	73.36	77.67	81.99	86.30
20-24	90.62	94.93	99.25	103.56	107.88
25-29	116.51	120.82	129.45	133.77	142.40
30-34	151.03	155.34	163.97	172.60	185.55
35-39	194.18	202.81	215.75	224.38	237.33
40-44	250.27	263.22	276.16	293.42	306.37
45-49	323.63	340.89	358.15	375.41	396.99
50-54	418.56	440.14	461.71	487.60	513.49
55-59	539.38	569.59	599.79	630.00	664.52
60-64	699.04	733.56	772.40	811.23	854.38
65-69	901.85	949.31	996.78	1052.88	1104.66
70-74	1165.07	1225.48	1290.21	1359.25	1428.29
75-79	1505.96	1583.63	1669.93	1756.23	1846.85
80-84	1946.10	2049.66	2157.53	2269.73	2390.55
85-89	2515.68	2645.14	2787.53	2934.25	3089.59
90-94	3249.25	3421.85	3603.08	3792.94	3991.44
95-99	4202.88	4422.94	4655.96	4901.92	5156.51
100-104	5428.35	5713.15	6015.20	6334.52	6666.78
105-109	7016.30	7387.39	7775.75	8185.68	8617.19
110-114	9070.27	9544.93	10049.79	10576.23	11137.19
115-119	11719.72	12336.78	12988.35	13670.13	14390.75
120-124	15150.20	15948.49	16785.61	17670.2	flyback
125-127	flyback	flyback	flyback		

## The IES instrument modes

These modes are described in [DOCUMENT\IES\\_MODES\IES\\_MODES.PDF](#).

### Calibrated data

Raw data (L2) are delivered to the archive. L2 may be the best data to use when looking for very weak signals or when the user wants to do some particular data processing before applying calibration factors. The team also delivers L3 data that are in the same form as the L2 data, but in units of differential flux (particles/ cm<sup>2</sup>/s/sr/eV). The L3 data have been processed to remove background. [Background data can be found in the CALIB\YYYY\MM\DD\ directories](#). L3 should in general be the preferred data for those who want to deal with the data in full detail.

### How to go from L2 to L3

In order to calculate differential fluxes from the raw count data, the geometric factor of the instrument is needed. The nominal geometric factor of IES is shown in Table 1. L3 data processing converts the data to physical units [particles/m<sup>2</sup>/s/sr/eV] by adjusting the geometric factor shown in Table 1 to account for the effects of the time resolution, summing of energy channels, summing of azimuth channels and summing of elevation channels as listed in [DOCUMENT\IES\\_MODES\IES\\_MODES.PDF](#). The conversion factor from counts to differential flux is given by:

$$GF \times (\Delta t/NS)(AS)(NA)(NE)/(effy),$$

where GF is the Geometric Factor,  $\Delta t$  is the length in seconds of a measurement interval, NS is the number of energy steps, AS is the number of adjacent azimuth steps, NE is the number of adjacent elevation steps, and effy is the counting efficiency. For example, for Mode 836 (electrons), the conversion from counts to differential flux is given by

$$(6.08 \times 10^{-5} \text{ cm}^2 \text{ sr eV/eV})(256 \text{ s}/126 \text{ energy steps})(2 \text{ adjacent energy steps})(2 \text{ adj. az. steps})(2 \text{ adj. elev. Steps})/(\text{counting efficiency}) = 1.98 \times 10^{-2} \text{ cm}^2 \text{ sr eV/eV}.$$

## Working with geometry data

### Coordinate systems

RPC-IES has a Cartesian instrument coordinate system, as illustrated in figure 1. The most natural description of the field of view is given by the angles corresponding to the sector and the elevation.

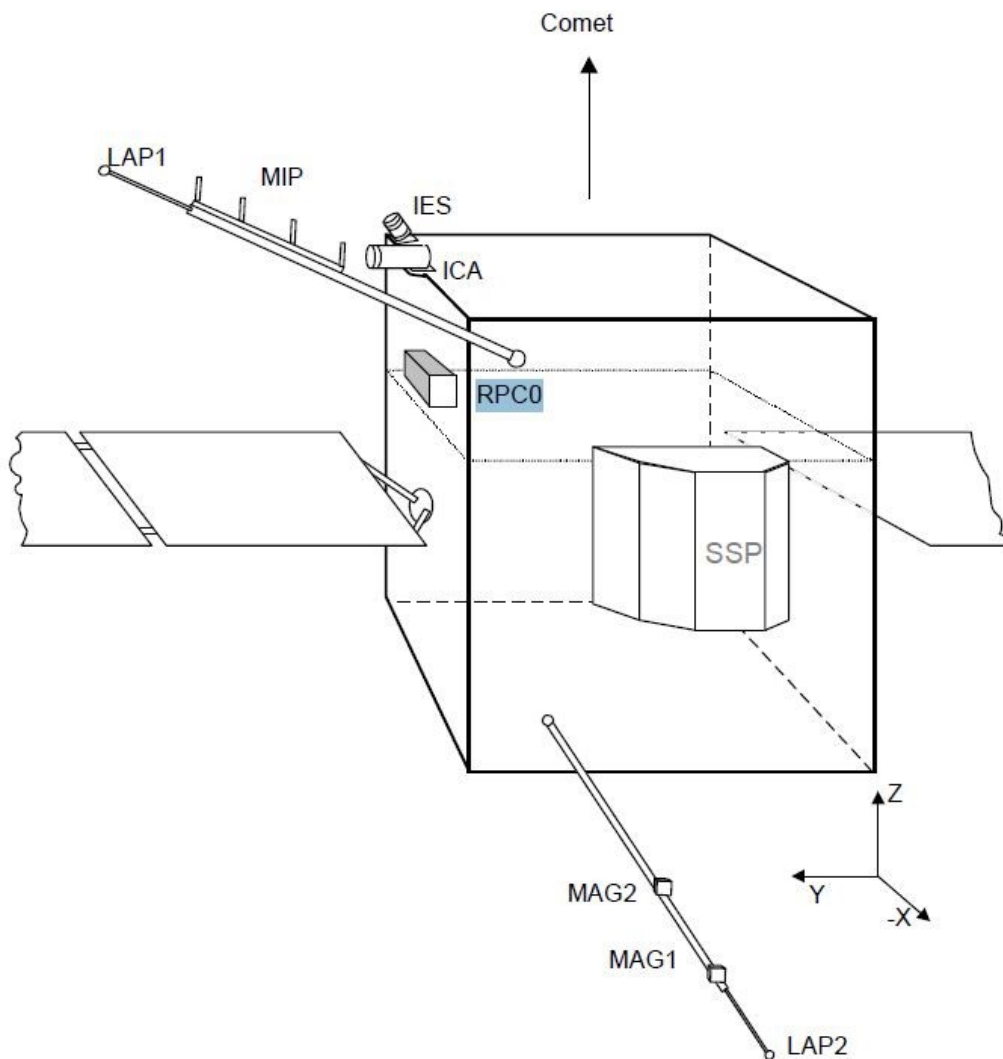


Figure 1. Illustration of the elements of RPC on the Rosetta spacecraft. The location of IES is shown in the top left of the figure.. The +Z axis is normally pointed to the comet and +X to the sun. However, science observations often result in different Rosetta attitudes, or, in fact, scanning.

If spice kernels are available to the user, the spacecraft reference frame can easily be turned into any suitable coordinate system, often CSEQ (Comet Sun Equatorial) is used. In the PSA L2 archive GEOM files are provided giving the position and spacecraft attitude in the local target coordinate system, CSEQ for comet 67P. The attitude is found as 3 unit vectors (spacecraft X, Y, Z) with each 3 components (CSEQ X, Y, Z), in positions 15 to 23 of the GEOM files. See data label or EAICD for more details. The spacecraft unit vectors can then be used to transform the data into the target frame, i.e. CSEQ for comet 67P.

### Working with the field of view

The field-of-view of RPC-IES is not complete. Part of the field of view is blocked by the spacecraft and instruments. RPC-IES typically had a free field-of-view

towards the sun and the comet. It is believed that much of the time the limited field-of-view was not a major problem. There are however clear cases when the spacecraft blocking of certain directions strongly influences the signal seen in the data. The FOV status at each time is given in the quality flag columns, i.e. whether there was no obstruction or some obstruction.

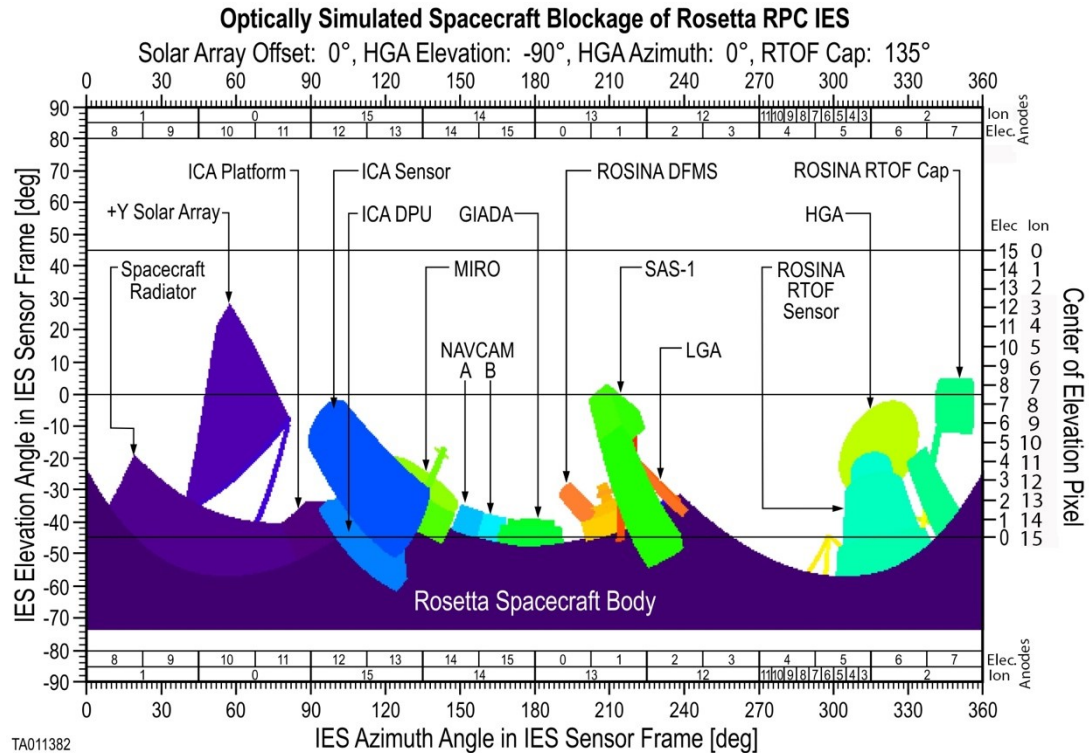


Figure 2 The RPC-IES field-of-view in spacecraft coordinates with known blockages (color-coded by object).

Figure 2 shows the field of view of RPC-IES as function of the azimuth angle (horizontal) and elevation angle. The Sun in a typical position is near azimuth of 300°, and the comet near 180°.

### Example of IES dataset

Examples of energy-time spectrograms for electrons and ions measured by RPC-IES on 30 July 2016 are shown in Fig. 3. Rosetta was ~ 3.5 au from the Sun and ~ 9 km from CG during this day. The electron population was primarily at energies < 200 eV. Higher count-rates are seen early in the day. The ion spectrogram shows the solar wind, with the protons at ~ 1 keV and alpha particles at twice that energy. A number of abrupt changes in energy appear. The band of very low energy (~ 10 eV) ions are locally ionized (e.g., water, CO<sub>2</sub>). Their high energies result from the negative spacecraft potential which attracts them. Note the abrupt changes in energy and intensity of both the electrons and ions. These are not unusual in the IES data and may be the result of fluctuations in the solar wind or other unknown effects. (The Rosetta attitude did not change significantly during this period.)

Figures 4 - 6 are line plots of the L5 moments data of this date. Compare the changes in the solar wind ion energy and density in Fig. 5 with the count-rates in Fig. 3.

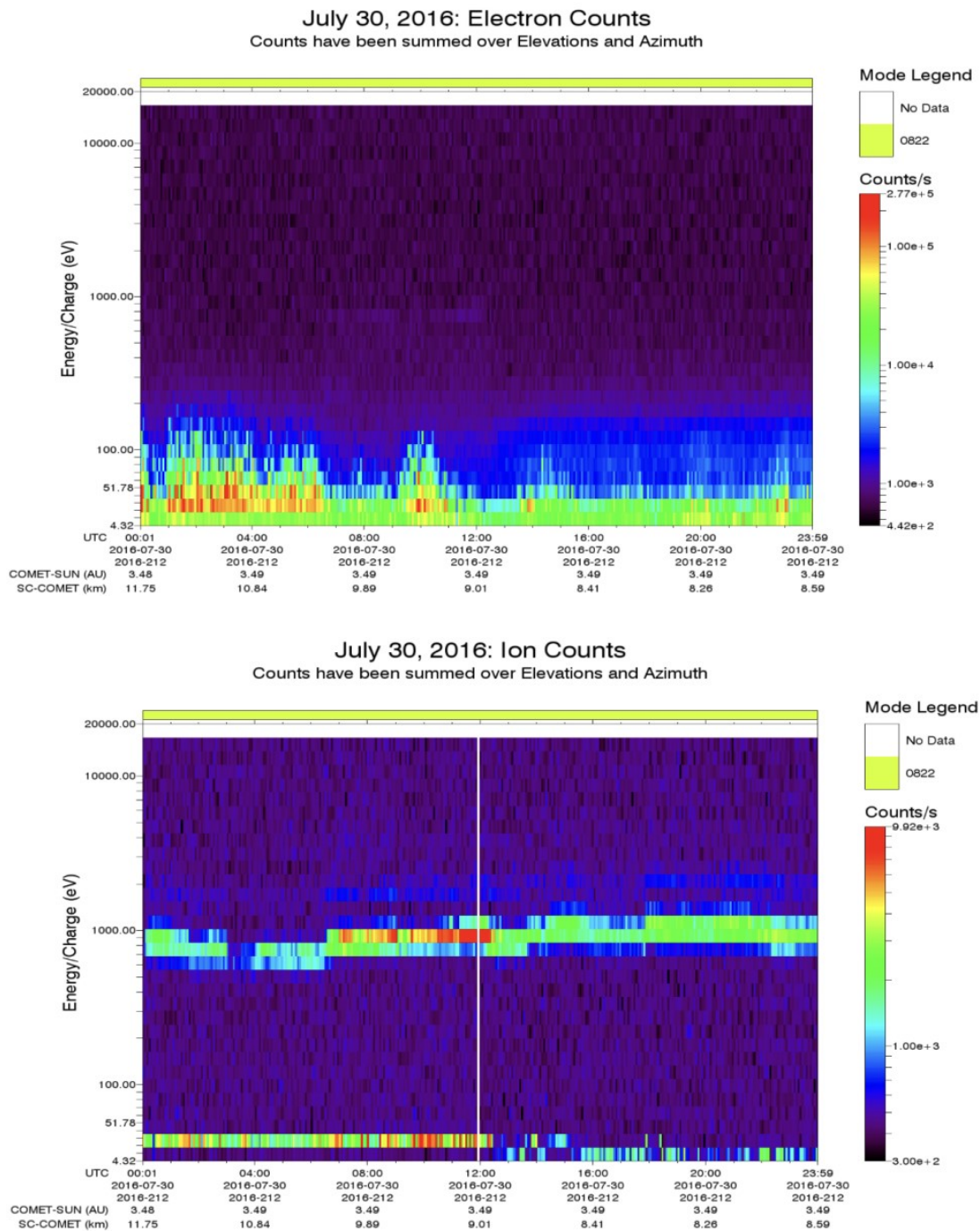


Figure 3: Energy-time spectrogram of electrons (upper) and ions (lower) on July 30, 2016.

## Appendix 1

### Contents of Level 2 data

The data files consist of 24 columns in two TAB files, one each for electrons and ions:

Column	Quantity	Example Data (Electrons)
1	SC EventTime (UTC)	2016-103T18:03:43.722
2	Mode	0836
3	Start Energy Step	0
4	End Energy Step	1
5	Start Elevation Angle Step	0
6	End Elevation Angle Step	1
7	Azimuth 00 (counts)	26.0000
8	Azimuth 01 (counts)	26.0000
9	Azimuth 02 (counts)	22.0000
10	Azimuth 03 (counts)	22.0000
11	Azimuth 04 (counts)	104.0000
12	Azimuth 05 (counts)	104.0000
13	Azimuth 06 (counts)	144.0000
14	Azimuth 07 (counts)	144.0000
15	Azimuth 08 (counts)	1.0000
16	Azimuth 09 (counts)	1.0000
17	Azimuth 10 (counts)	0.0000
18	Azimuth 11 (counts)	-1.0000
19	Azimuth 12 (counts)	-1.0000
20	Azimuth 13 (counts)	1.0000
21	Azimuth 14 (counts)	2.0000
22	Azimuth 15 (counts)	2.0000
23	Cycle Duration (seconds)	256
24	Quality Flags	00100

Column	Quantity	Example Data (Ions)
1	SC EventTime (UTC)	2016-103T00:18:43.722
2	Mode	0836
3	Start Energy Step	0
4	End Energy Step	1
5	Start Elevation Angle Step	0
6	End Elevation Angle Step	1
7	Azimuth 00 (counts)	1.0000
8	Azimuth 01 (counts)	0.0000
9	Azimuth 02 (counts)	2.0000
10	Azimuth 03 (counts)	0.1111
11	Azimuth 04 (counts)	0.1111
12	Azimuth 05 (counts)	0.1111
13	Azimuth 06 (counts)	0.1111
14	Azimuth 07 (counts)	0.1111
15	Azimuth 08 (counts)	0.1111
16	Azimuth 09 (counts)	0.1111
17	Azimuth 10 (counts)	0.1111
18	Azimuth 11 (counts)	0.1111
19	Azimuth 12 (counts)	1.0000
20	Azimuth 13 (counts)	1.0000
21	Azimuth 14 (counts)	1.0000
22	Azimuth 15 (counts)	2.0000
23	Cycle Duration (seconds)	256
24	Quality Flags	00000

### Contents of L3 data

The L3 data format is identical to L2 data except that instead of counts the entries are given in differential energy flux [ $\text{eV/s/cm}^2/\text{sr}/\text{eV}$ ].

A description of the flux calculation is contained in:

### Contents of L4 data

Level 4 data are not produced for IES.

### Contents of L5 data

L5 data are produced by numerical moment calculation from the L3 data and give density, speed, and temperature for all species measured. As example, Fig. 3 shows line plots of these parameters for electrons for 30 July 2016. Figure 4 gives the same parameters for solar wind protons on the same date and fig. 5 does likewise for solar wind alphas. These line plots are useful for getting a quick view of the data for a particular date. Note that these moment calculations are affected by the limited FOV of IES and that the L3 data have not been corrected for the spacecraft potential. See also alternative plasma measurements from other RPC instruments given in the RPC UG.

A description of the moment calculation is contained in:

DOCUMENT\MOMENTS\_CALCULATION\MOMENTS\_CALCULATION.PDF

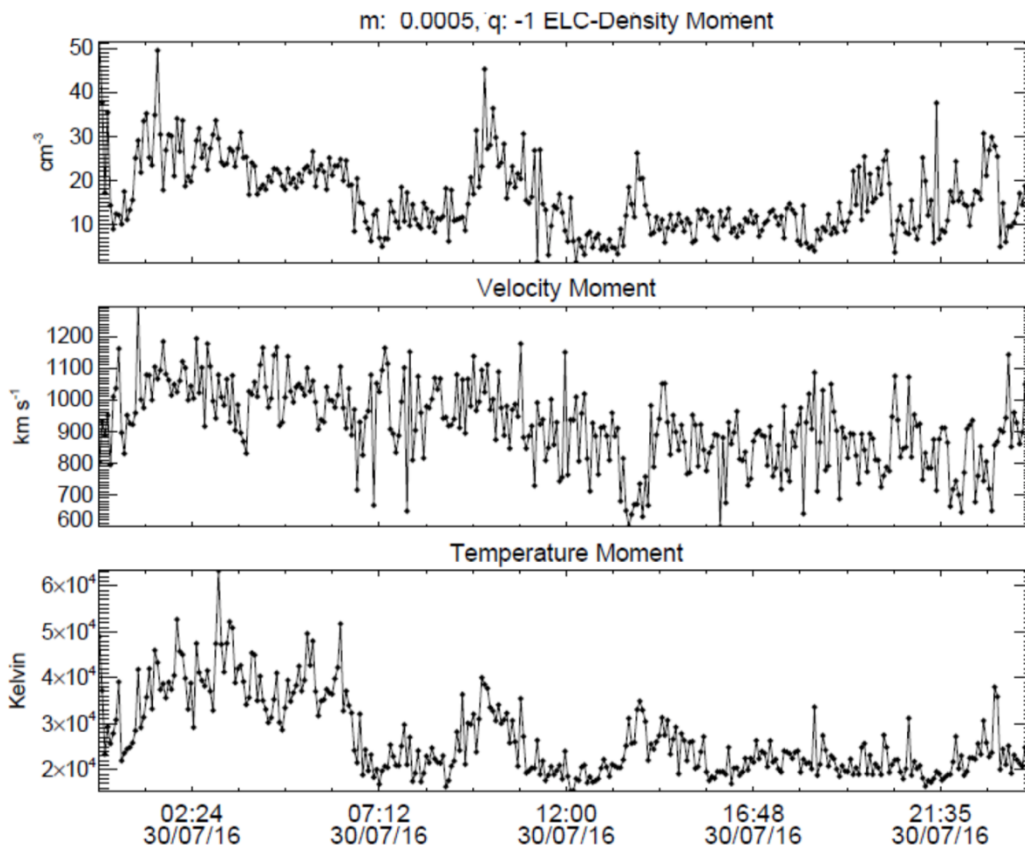


Figure 4. Line plots of result of moment calculations for electrons measured on 30 July 2016.

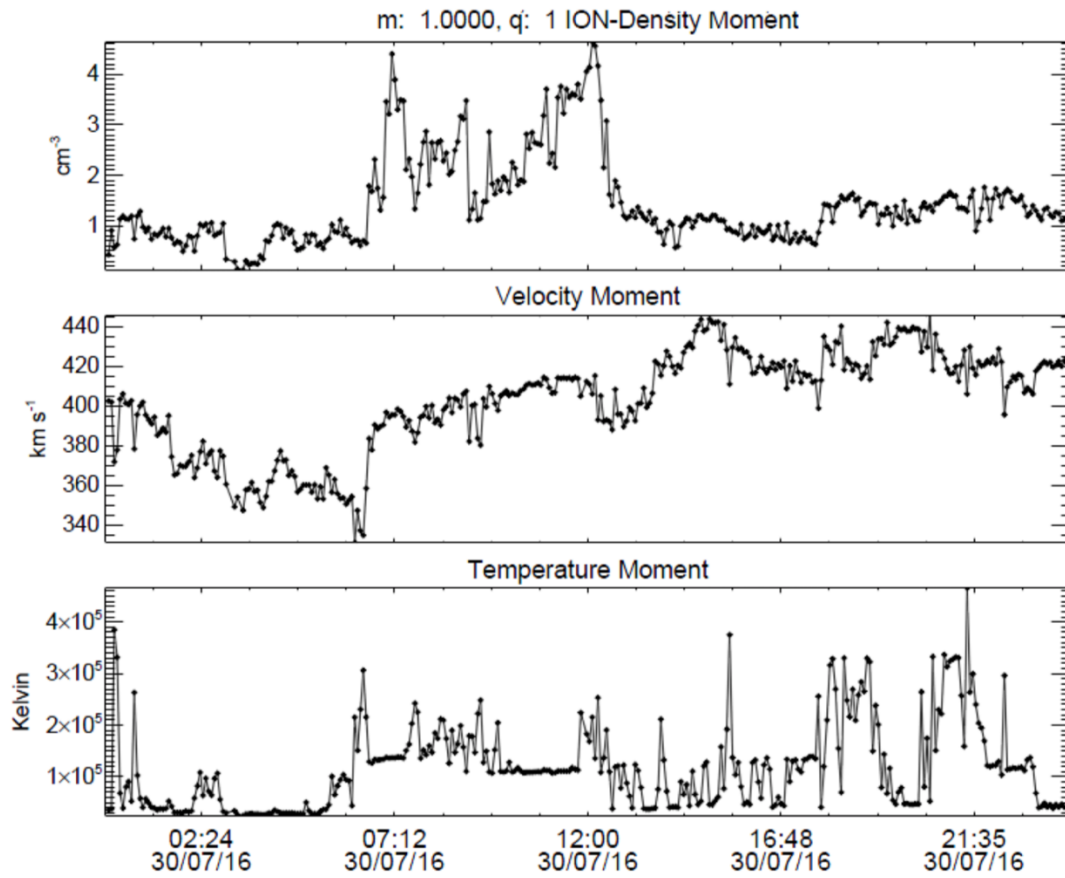


Figure 5. Line plots of result of moment calculations for protons measured on 30 July 2016.

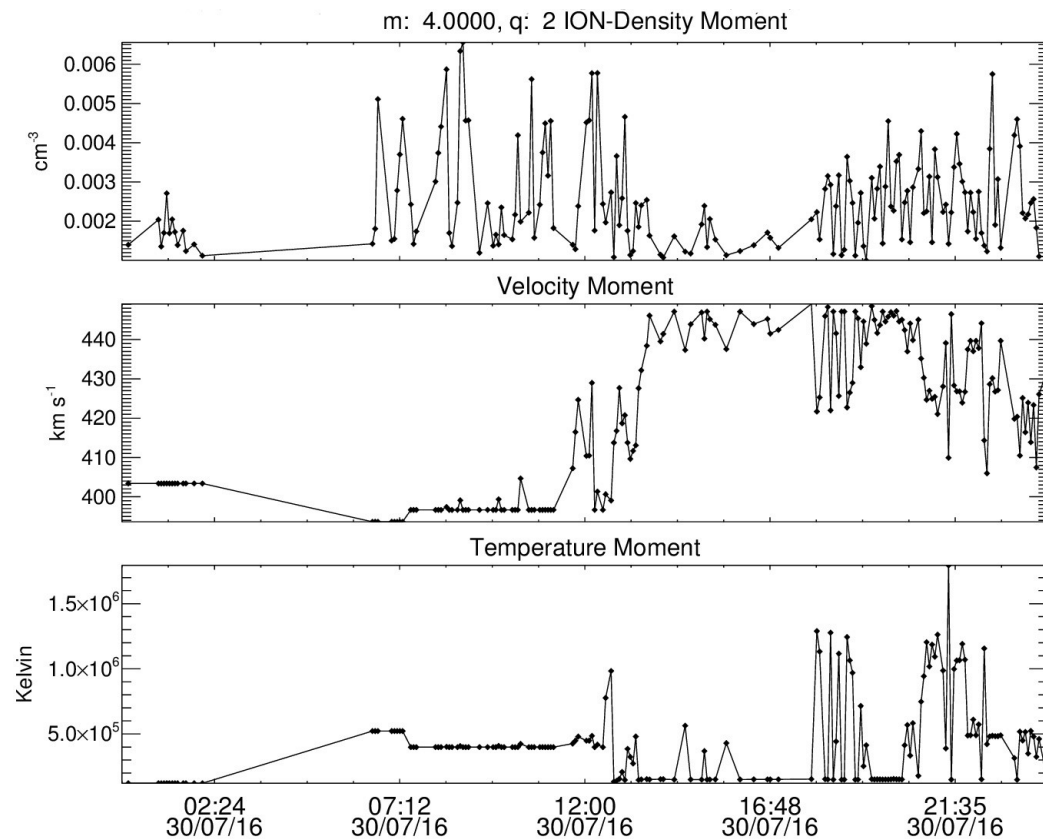


Figure 6. Line plots of result of moment calculations for alpha particles measured on 30 July 2016. The gaps are due to very low count rates during those periods.

## References

- Broiles, T. W., J. L. Burch, G. Clark, C. Koenders, E. Behar, R. Goldstein, S. A. Fuselier, P. Mokashi and M. Samara, Rosetta observations of solar wind interaction with the comet 67P/Churyumov-Gerasimenko, *Astron. Astrophys*, 583, doi: 10.1051/0004-6361/201526046, 2015.
- Burch, J. L., Goldstein, R., Cravens, T. E., et al. 2007, *Space Sci. Rev.*, 128, 697.
- Burch, J. L., T. E. Cravens, K. Llera, R. Goldstein, P. Mokashi, C.-Y. Tzou, and T. Broiles (2015a), Charge exchange in cometary coma: Discovery of H<sup>-</sup> ions in the solar wind close to comet 67P/Churyumov-Gerasimenko, *Geophys. Res. Lett.*, 42, 5125–5131, doi: 10.1002/2015GL064504.
- Burch, J. L., T. I. Gombosi, G. Clark, P. Mokashi, and R. Goldstein (2015b), Observation of charged nanograins at comet 67P/Churyumov-Gerasimenko, *Geophys. Res. Lett.*, 42, 6575–6581, doi: 10.1002/2015GL065177.
- Carr, C., Cupido, E., Lee, C. G. Y., et al. 2007, *Space Sci. Rev.*, 128, 629
- Clark, G., T. W. Broiles, J. L. Burch, G. A. Collinson, T. Cravens, R. A. Frahm, J. Goldstein, R. Goldstein, K. Mandt, P. Mokashi, M. Samara and C. J. Pollock (2015), Goldstein, R., J. L. Burch, P. Mokashi, T. Broiles, K. Mandt, J. Hanley, T. Cravens, A. Rahmati, M. Samara, G. Clark, M. Hässig, and J. M. Webster (2015), The Rosetta Ion and Electron Sensor (IES) measurement of the development of pickup ions

from comet 67P/Churyumov-Gerasimenko. *Geophys. Res. Lett.*, 42, 3093–3099.  
doi: 10.1002/2015GL063939.

Eriksson, A. I., Boström, R., Gill, R., et al. 2007, *Space Sci. Rev.*, 128, 729

Glassmeier, K.-H., Richter, I., Diedrich, A., et al. 2007, *Space Sci. Rev.*, 128, 649.

Nilsson, H. et al., 2007, *Space Sci. Rev.*, 128, 671.

Trotignon, J. G., Michau, J. L., Lagoutte, D., et al. 2007, *Space Sci. Rev.*, 128, 713